nature portfolio

Peer Review File

Escalating Transmissibility of SFTS in High-Endemic China

Corresponding Author: Dr Tianmu Chen

This file contains all reviewer reports in order by version, followed by all author rebuttals in order by version.

Version 0:

Reviewer comments:

Reviewer #1

(Remarks to the Author)
In this study, the authors claimed to investigate the cross-species transmission dynamics of SFTS among 'human-tick-animal host' populations using a Multi-Population and Multi-Route Dynamic Model. However, they mainly concentrated on the human population, and it is not clear among 3883 reported cases how many cases were infected by contact with animal and ticks respectively. They claimed they had used model fit to estimate the transmission rate beta1, but their method and results of model fit are lacking. They also claimed that next-generation matrix was used to calculate reproduction number, I cannot follow how this was done.

Other minors
In Introduction, some introduction about epidemiology and transmission mode of SFTS should be given. severity? reporting rate? hospitalization and deaths?
More information about 'human-tick-animal host' populations.

Line 91: "parameters from existing literature," can values of all parameters be borrowed from literature? Are they relevant?
Table 1: are there any uncertainties among these estimates of model parameters? If yes, how robust are your conclusions? Some probabilistic sensitivity analyses should be conducted.

Table 2: the values listed in the last row are not all "Total"
The uncertainty in "Total" should be listed.

Could the high incidence from 2023 be linked to the NPIs against COVID-19 in China?

Reviewer #2

(Remarks to the Author)
This is a very good manuscript that describes a new model for SFTS in China. This disease is undergoing a rapid expansion and needs better study, so this paper is very timely. The authors do a very good job of presenting much of the information and results. I have only a couple majors comments and a few minor corrections to suggest.

Major comments.
1. I am a bit concerned about the minimal amount of information in the text about the tick vector itself. Since this population is included in the equations, I would suggest that there is a need to have a bit more about the biology of this tick species and its life history described in the introduction. For example, what is known about any recent changes in this ticks geographic range or population density? With a weekly time step, the tick life history dynamics might play a larger role than is currently included with this model.
2. Figure 3 and 4 are overly complicated. While I appreciate the amount of information provided, there is so much there it is overwhelming and impossibly small font. I would recommend the authors either divide up the information into a series of figures or move some of these to the supplemental information. Either way, these need to be simplified. Additionally, all figures should have more information in the captions to tell the reader what is being shown and the interpretations of those findings.

Other smaller comments.
1. The language of lines 330-333 is a bit confusing. I would suggest rewording to better explain that the drop of Re below one starts during the windows given. As it currently reads, it would seem that these were the only weeks that it was below 1.
2. Spacing needs fixed in line 354.
3. Numbering of list in lines 424-431 is not a usual numbering style.
4. Coloring for Figure 7 is a bit confusing. I associate green with Re < 1 and red with Re > 1 as some type of danger indication, but this seems to just be colored by region? It would be easier to interpret if the color scheme was based on the Re value.

Reviewer #3

(Remarks to the Author)
I co-reviewed this manuscript with one of the reviewers who provided the listed reports. This is part of the Nature Communications initiative to facilitate training in peer review and to provide appropriate recognition for Early Career Researchers who co-review manuscripts.

Version 1:

Reviewer comments:

Reviewer #1

(Remarks to the Author)
Thank authors for taking effort to thoroughly revise their manuscript. Although it improves in many aspects, I still have concerns about how they conducted model fit with many things unknown, for example

1/ Their formula for Re (actually R0 because they calculated it on the disease-free equilibrium) is involved with population size N1, N2 and N3. Without the values of these, how to calculate Re? if the values of N1, N2 and N3 were used, how were the populations estimated?

2/ as humans can be infected via contact with humans, ticks and animals, what are the corresponding proportions of the infections? Does this agree with the data listed in Table 2? This knowledge may provide some key information for the control of the disease.

(Remarks on code availability)

Version 2:

Reviewer comments:

Reviewer #1

(Remarks to the Author)
The authors have satisfactorily addressed my second concern, but I am still not clear how N2 and N3 are jointly estimated. In the revised version, they stated
"In the calibration procedure, the parameters governing the magnitude and timing of this seasonal pattern (denoted $\beta 0$ and α), together with the effective host population sizes associated with tick-mediated transmission pathways (N2 and N3), were treated as free parameters and jointly estimated"

for this they justified as
"...the plausible ranges of N2 and N3 were constrained according to the scale of the human population N1 in each study area, in order to preserve realistic orders of magnitude and prevent implausible parameter combinations"

" N2 and N3 are pathway-scaling parameters that were jointly estimated together with the transmission parameters, with their plausible ranges constrained according to the scale of N1 in each study area, rather than being treated as fixed demographic quantities"

If constrained, they could not be free.
Even if "jointly estimated", I cannot follow how this was done.

(Remarks on code availability)

We thank all three reviewers for their prompt, thorough, and constructive feedback on this manuscript. In responding to these reviews, we have made substantial changes to the manuscript text to address the points raised by reviewers. Please find the comments and our responses reproduced below. Author responses are in blue.

Reviewer #1 (Remarks to the Author):

In this study, the authors claimed to investigate the cross-species transmission dynamics of SFTS among 'human-tick-animal host' populations using a Multi-Population and Multi-Route Dynamic Model. However, they mainly concentrated on the human population, and it is not clear among 3883 reported cases how many cases were infected by contact with animal and ticks respectively. They claimed they had used model fit to estimate the transmission rate beta1, but their method and results of model fit are lacking. They also claimed that next-generation matrix was used to calculate reproduction number, I cannot follow how this was done.

Author's Response：

We are grateful to the reviewer for this important comment, which has helped us strengthen the clarity and rigor of the manuscript. We agree that the reviewer's concern about case-level exposure attribution is particularly important. To address this point as clearly as possible, we have added and summarized the available exposure history information of the reported cases, so that the currently missing or incomplete route-specific details are presented more transparently and the evidence base for cross-species transmission is more clearly documented. In addition, we expanded the description of the model fitting strategy and provided corresponding results to improve transparency in the estimation of key transmission parameters. Finally, we clarified the derivation of the reproduction number using the next-generation matrix, adding intermediate steps and explanations to improve readability.

To address this major comment comprehensively, we provide point-by-point responses to each component of the reviewer's concern below.

However, they mainly concentrated on the human population, and it is not clear among 3883 reported cases how many cases were infected by contact with animal and ticks respectively.

Author's Response：

Among 3,883 reported SFTS cases in Anhui Province, local CDC staff documented detailed exposure histories for 1,720 cases.. The exposure history records compiled information regarding tick exposure, animal related contact and close contact with symptomatic individuals, together with specific items such as type of residence, outdoor activities prior to onset, presence and sighting of ticks in the environment, history of tick bite, skin breaks, contact with individuals with similar symptoms, household animal keeping and contact with wild animals, all collected using a uniform investigation form.

As you suggested, we have now added a summary of the exposure-history findings：

Revised version: Lines 374-389; Clean version: Lines 188-203：

Among 3,883 reported cases, 1,720 completed a standardized on-site questionnaire, which documented detailed pre-onset exposure histories (including pre-onset outdoor activity history, tick bite history, etc.).

The results indicated that the primary pre-onset exposures were related to agricultural and forestry outdoor activities. These included farming (60.9%), grass cutting (23.6%), and tea picking (10.4%). Epidemiological investigations revealed that, among cases aware of their environmental context, a significant proportion reported the presence of ticks in their residential environment (41.4%) and a clear history of tick bites (43.9%). Furthermore, keeping animals at home (46.5%) was also a common exposure factor. Notably, although at lower proportions, the investigation also revealed instances of contact with similar patients (2.7%), as well as the presence of skin breaks (11.5%) prior to onset, which may represent non-vector transmission routes facilitating viral entry (Table 2).

Table 2 Exposure history among 1,720 SFTS cases with detailed field investigations in Anhui Province

Exposure History	Number of Cases (n)	Proportion (%)
Type of Residence		
Hilly or mountainous area	1128	65.6

Plain and other types	592	34.4
Outdoor Activities Prior to Onset	0	
Farming	1047	60.9
Tea picking	179	10.4
Grass cutting	406	23.6
Herding/Livestock grazing	13	0.8
Logging	46	2.7
Hunting	4	0.2
Tourism	15	0.9
Presence of Ticks in the Residential Environment		
Yes	532	30.9
No	162	9.4
Unknown	1026	59.7
Sighting of Ticks		
Yes	375	21.8
No	531	30.9
Unknown	814	47.3
History of Tick Bite Prior to Onset		
Yes	329	19.1
No	421	24.5
Unknown	970	56.4
Presence of Skin Breaks Prior to Onset		
Yes	197	11.5
No	1523	88.5
Contact with Individuals with Similar Symptoms Prior to Onset		
Yes	46	2.7
No	1674	97.3
Household animal keeping		
Yes	735	42.7
No	844	49.1
Unknown	141	8.2
Contact with Wild Animals Prior to Onset		
Yes	8	0.5
No	1457	84.7
Unknown	255	14.8

Because tick exposure, animal contact and human contact may occur simultaneously in the same individual and detailed investigations are only available for a subset of reported cases, it is not possible to assign every infection unambiguously to a single

route. We therefore do not report precise route specific case counts for all 3,883 patients and instead use these empirical patterns to justify the inclusion of multiple transmission pathways in the model; we also explicitly acknowledge in the revised Discussion that the partial coverage of detailed field investigations and overlapping exposures limits our ability to distinguish infections acquired via tick, animal and human routes.

We appreciate your valuable comments, which have made our study more comprehensive.

They claimed they had used model fit to estimate the transmission rate beta1, but their method and results of model fit are lacking.

Author's Response：

We appreciate the suggestions you put forward. Indeed, as you noted, adding the fitting methods and corresponding results will make the findings of our manuscript more comprehensive and complete.

We have revised the manuscript to provide a clearer and more transparent description of the parameter fitting strategy and its results. Specifically, we added a dedicated Section 2.4.1 Parameter Fitting (lines 240-273) to explain in detail how the human-to-human transmission coefficient β_1 was estimated. We used Python to fit the human component of the multi-population model to the observed weekly SFTS incidence. The ODE system was numerically solved, and β_1 was estimated by minimizing the sum of squared differences between model-predicted and observed weekly new human cases under biologically plausible box constraints. All other natural history and demographic parameters were fixed based on published literature and local epidemiological data.

To ensure that the fitting procedure and its performance are clearly documented and reproducible, we now report standard goodness-of-fit metrics, including R^2, MSE, RMSE, and MAE, in the revised text and in Supplementary Material Appendix Table S5. For the reviewer's convenience, we also provide Table S6 below together with the corresponding revised manuscript text.

Revised version: Lines 749-769; Clean version: Lines 550-570：

Parameter Fitting was conducted in Python 3.10.13. Given the low and highly sporadic daily number of reported SFTS cases in Anhui Province, the surveillance data were aggregated to weekly incidence to reduce stochastic noise and obtain a smoother epidemic trajectory. The weekly number of confirmed human SFTS cases in each study area was used as the calibration target. The deterministic model was integrated with a fourth-order Runge–Kutta scheme using a weekly time step and a relative tolerance of 0.001.

The human-to-human transmission coefficient β_1 is specified as a seasonal function of time and is parameterized by a baseline intensity, a phase parameter and a period. In the calibration procedure, the parameters governing the magnitude and timing of this seasonal pattern (denoted β_0 and α) were treated as free transmission parameters, whereas the period T and all remaining natural-history and demographic parameters were fixed at the baseline values listed in Table 1. For each study area, β_0 and α were estimated by nonlinear least squares, which minimizing the sum of the squared differences between the observed weekly incidence and the model-predicted weekly number of new symptomatic infections. The optimization was implemented in Python using a standard nonlinear least-squares routine (lmfit package), and convergence was assessed by the relative change in the objective function. The goodness-of-fit of the calibrated model is summarized in the Results and in Supplementary material Appendix Table S5 using the coefficient of determination (R2), mean squared error (MSE), and mean absolute error (MAE) between observed and model-predicted weekly cases.

Supplementary Material:

Table S5 Goodness-of-fit metrics for model fitting of weekly SFTS incidence by region and year in Anhui Province

Region	Year	MSE	RMSE	R_squared	P	MAE
Anhui	2023	126.4771	11.2462	0.7533	＜0.05	9.1203
Anhui	2022	75.3540	8.6807	0.7518	＜0.05	6.6896
Anhui	2021	28.6723	5.3547	0.6762	＜0.05	4.2174
Anhui	2020	34.5671	5.8794	0.7343	＜0.05	4.5124
Anhui	2019	21.8073	4.6698	0.6500	＜0.05	3.4778
Anqing	2023	6.2806	2.5061	0.4036	＜0.05	1.7340
Anqing	2022	3.2783	1.8106	0.5761	＜0.05	1.3476

Anqing	2021	2.3109	1.5202	0.2180	＜0.05	1.1453
Anqing	2020	3.6064	1.8991	0.5507	＜0.05	1.3488
Anqing	2019	4.2093	2.0516	0.2027	＜0.05	1.4398
Chuzhou	2023	13.4682	3.6699	0.5931	＜0.05	2.8005
Chuzhou	2022	13.4512	3.6676	0.6522	＜0.05	2.7858
Chuzhou	2021	11.1183	3.3344	0.3878	＜0.05	2.6212
Chuzhou	2020	8.7796	2.9630	0.3675	＜0.05	2.3792
Chuzhou	2019	2.2676	1.5058	0.5097	＜0.05	1.1458
Hefei	2023	17.3490	4.1652	0.5528	＜0.05	2.8642
Hefei	2022	7.5922	2.7554	0.5404	＜0.05	1.9978
Hefei	2021	4.8321	2.1982	0.3085	＜0.05	1.7529
Hefei	2020	2.6676	1.6333	0.5628	＜0.05	1.2628
Hefei	2019	2.3616	1.5367	0.1946	＜0.05	1.1082
Lu'an	2023	8.6658	2.9438	0.5337	＜0.05	2.0972
Lu'an	2022	4.2575	2.0634	0.4320	＜0.05	1.4700
Lu'an	2021	2.2641	1.5047	0.2003	＜0.05	1.2094
Lu'an	2020	2.8781	1.6965	0.3804	＜0.05	1.3476
Lu'an	2019	3.2344	1.7985	0.4423	＜0.05	1.3984
Ma'anshan	2023	2.2135	1.4878	0.5784	＜0.05	1.2566
Ma'anshan	2022	3.9523	1.9880	0.5376	＜0.05	1.3542
Ma'anshan	2021	1.8192	1.3488	0.1620	＜0.05	0.9948
Ma'anshan	2020	2.3401	1.5297	0.1814	＜0.05	1.1490
Ma'anshan	2019	0.6256	0.7910	0.1805	＜0.05	0.6059

They also claimed that next-generation matrix was used to calculate reproduction number, I cannot follow how this was done.

Author's Response：

We appreciate your sincere suggestions. Indeed, we omitted the derivation process of the next-generation matrix method in the main text of our manuscript, and we have now supplemented it in accordance with your recommendations.

We have expanded the description of the derivation of the reproduction number in the revised Methods **Section 2.4.2 "Calculation of the Reproduction Number R_e"**. We now explicitly define the vector of infected compartments across humans, ticks and animal hosts, construct the new infection matrix $\underline{F}$ and the transition matrix V by linearising the full model at the disease free equilibrium, and state that the reproduction number is given by the dominant eigenvalue of the next generation matrix. These additions are intended to make the use of the next generation matrix in

our multi population, multi route framework fully transparent to readers.

Revised version: Lines 784-807; Clean version: Lines 585-608：

The model defines the total human population as $N_1=S_1+E_1+A_1+I_1+R_1$, the total tick population as $N_2=S_2+E_2+A_2$, and the total host animal population as $N_3=S_3+E_3+A_3$. Disease-free equilibrium (DFE) represented by $E_0=(N_1,0,0,0,0,N_2,0,0,N_3,0,0)$, in which $E_{01}=(N_1,0,0,0,0)$, $E_{02}=(N_2,0,0)$ and $E_{03}=(N_3,0,0)$. Using the next-generation matrix approach, the differential equations for the infectious compartments E_1, A_1, I_1, E_2, A_2, $E_3$and A_3 are decomposed into the inflow matrix F and the outflow matrix V:

$$\frac{d}{dt}\begin{bmatrix} E_1 \\ A_1 \\ I_1 \\ E_2 \\ A_2 \\ E_3 \\ A_3 \end{bmatrix} = \mathrm{F}\text{-}V$$

$$= \begin{bmatrix} \beta_1 S_1(I_1+kA_1)+\beta_{2\text{-}1}S_1A_2+\beta_{3\text{-}1}S_1A_3 \\ 0 \\ 0 \\ \beta_{3\text{-}2}S_2A_3 \\ 0 \\ \beta_{2\text{-}3}S_3A_2 \\ 0 \end{bmatrix} - \begin{bmatrix} d_{r1}E_1+\omega_1E_1 \\ -p\omega_1E_1+d_{r1}A_1+\gamma' A_1 \\ -(1\text{-}p)\omega_1E_1+\gamma I_1+(d_{r1}+f)I_1 \\ d_{r2}E_2+\omega_2E_2 \\ -\omega_2E_2+d_{r2}A_2 \\ d_{r3}E_3+\omega_3E_3 \\ -\omega_3E_3+d_{r3}A_3 \end{bmatrix}.$$

Taking the partial derivatives with respect to each infectious compartment, we obtain the Jacobian matrices of $\mathcal{F}$ and $\mathcal{V}$ at the DFE as follows:

$$F(E_0) = \begin{pmatrix} 0 & \beta_1N_1k & \beta_1N_1 & 0 & \beta_{2-1}N_1 & 0 & \beta_{3-1}N_1 \\ 0 & 0 & 0 & 0 & 0 & 0 & 0 \\ 0 & 0 & 0 & 0 & 0 & 0 & 0 \\ 0 & 0 & 0 & 0 & 0 & 0 & \beta_{3-2}N_2 \\ 0 & 0 & 0 & 0 & 0 & 0 & 0 \\ 0 & 0 & 0 & 0 & \beta_{2-3}N_3 & 0 & 0 \\ 0 & 0 & 0 & 0 & 0 & 0 & 0 \end{pmatrix},$$

$$V(E_0) = \begin{pmatrix} d_{r1}+\omega_1 & 0 & 0 & 0 & 0 & 0 & 0 \\ -p\omega_1 & d_{r1}+\gamma' & 0 & 0 & 0 & 0 & 0 \\ -(1-p)\omega_1 & 0 & \gamma+d_{r1}+f & 0 & 0 & 0 & 0 \\ 0 & 0 & 0 & d_{r2}+\omega_2 & 0 & 0 & 0 \\ 0 & 0 & 0 & -\omega_2 & d_{r2} & 0 & 0 \\ 0 & 0 & 0 & 0 & 0 & d_{r3}+\omega_3 & 0 \\ 0 & 0 & 0 & 0 & 0 & -\omega_3 & d_{r3} \end{pmatrix}.$$

Further solving for the inverse matrix of $V(E_0)$ yields:

$$V(E_0)^{-1} = \begin{pmatrix} \frac{1}{d_{r1}+\omega_1} & 0 & 0 & 0 & 0 & 0 & 0 \\ \frac{p\omega_1}{(d_{r1}+\omega_1)(d_{r1}+\gamma')} & \frac{1}{d_{r1}+\gamma'} & 0 & 0 & 0 & 0 & 0 \\ \frac{(1-p)\omega_1}{(d_{r1}+\omega_1)(\gamma+d_{r1}+f)} & 0 & \frac{1}{\gamma+d_{r1}+f} & 0 & 0 & 0 & 0 \\ 0 & 0 & 0 & \frac{1}{d_{r2}+\omega_2} & 0 & 0 & 0 \\ 0 & 0 & 0 & \frac{\omega_2}{(d_{r2}+\omega_2)d_{r2}} & \frac{1}{d_{r2}} & 0 & 0 \\ 0 & 0 & 0 & 0 & 0 & \frac{1}{d_{r3}+\omega_3} & 0 \\ 0 & 0 & 0 & 0 & 0 & \frac{\omega_3}{(d_{r3}+\omega_3)d_{r3}} & \frac{1}{d_{r3}} \end{pmatrix}.$$

Then, the effective reproduction number R_e of the model is the spectral radius of the next generation matrix $FV(E_0)^{-1}$. Direct calculation gives

$$R_e = \rho(FV(E_0)^{-1})$$

$$= max\left\{ \frac{p\omega_1\beta_1 N_1 k}{(d_{r1}+\omega_1)(d_{r1}+\gamma')} + \frac{(1-p)\omega_1\beta_1 N_1}{(d_{r1}+\omega_1)(\gamma+d_{r1}+f)}, \sqrt{\frac{\omega_2\beta_{2\text{-}3}N_3\omega_3\beta_{3\text{-}2}N_2}{(d_{r2}+\omega_2)d_{r2}(d_{r3}+\omega_3)d_{r3}}} \right\}.$$

Other minors

In Introduction, some introduction about epidemiology and transmission mode of SFTS should be given. severity? reporting rate? hospitalization and deaths?

More information about ‘human-tick-animal host' populations.

Author’s Response：

We sincerely thank the reviewer for this valuable suggestion, which has helped to make our introduction more comprehensive and detailed.

Following the reviewer's advice, we have enhanced the Introduction section by adding descriptions of the clinical features and key epidemiological indicators of SFTS, as well as refining the information about ‘human-tick-animal host' populations.. Specifically, the following text has been added:

Revised version: Lines 61-64; Clean version: Lines 51-54：

SFTS is a tick-borne disease for which the causative agent is the SFTS virus (SFTSV). Illness typically presents with a constellation of clinical features including fever, thrombocytopenia, leukopenia, alongside central nervous system involvement and gastrointestinal symptoms.

Revised version: Lines 67-70; Clean version: Lines 57-60：

A 2024 review and meta-analysis reported a notification rate for SFTS of 18.59 (95% CI: 16.68–20.72) per 10 million persons, with a notification–deaths rate of 3.51 (95% CI: 2.97–4.13) per 10 million persons. The case–fatality rate was 7.40% (95% CI: 6.64–8.25) in China

Revised version: Lines 75-91; Clean version: Lines 65-81：

Ticks, including species such as *Haemaphysalis longicornis* and *Haemaphysalis flava*, are established as the primary vectors for SFTSV transmission. *Haemaphysalis longicornis* is extensively distributed and potentially affects 588 million people across 1,140 counties in China. Furthermore, its distribution range within China may be continually expanding. Study has demonstrated that all developmental stages of *H. longicornis* can acquire SFTSV by infecting animals through biting, and subsequently transmit the virus back to naive animals during blood-feeding. Following SFTSV infection at any single developmental stage, transstadial transmission of the virus to the subsequent developmental stage was observed. Female adult ticks are capable of vertical virus transmission via the transovarial route. Collectively, these results confirm that SFTSV can undergo both transstadial and transovarial transmission, thereby establishing a complete transmission cycle spanning the *H. longicornis* larvae–nymphs–adults life cycle and animal hosts. Additionally, the virus also exhibits a broad animal host tropism, infecting species such as cats, cattle, sheep, and hedgehogs,

thereby establishing a risk of zoonotic transmission. Evience of human-to-human spread has also been documented. The extensive host range coupled with multiple transmission pathways presents a multifaceted challenge for public health control efforts.

Line 91: “parameters from existing literature,” can values of all parameters be borrowed from literature? Are they relevant?

Author’s Response：

We sincerely thank the reviewer for this valuable suggestion, which has helped us refine the description of our parameter sources and improve the clarity of the Methods section. We agree that our original wording may have implied that all parameter values were derived from existing literature, which was an imprecise expression. To address this, we have revised the relevant statement in the manuscript.

Revised version: Lines 605-607; Clean version: Lines 406-408：

The revised text now reads: “and epidemiological parameters derived from official statistics and relevant published studies (Table 3)”, which clarifies that our parameterisation is based on a combination of official data sources and published evidence rather than literature alone.

To further strengthen the linkage between parameter values and their supporting evidence, and to better facilitate the planned probabilistic sensitivity analysis (PSA), we have expanded the number of references for model parameters on the existing basis. These updates are reflected in the revised Table 2.

Revised version: Line 746; Clean version: Lines 547：

Table 3. Parameter definitions and numerical values for MMDM

Parameter	Definition	Value	Range	Unit	Source
Person					
β_1	Person-to-person transmissibility	-	-	$(\text{Person}*\text{week})^{-1}$	Model fitting

	coefficient				
κ	Relative transmissibility coefficient of unapparent infection	1	-	1	-
p	Proportion of latent infection	0.043	0.00023–0.0917	1	Ref.[10,41,42]
$1/\omega_1$	Incubation period	1.57	1.28571–2.14286	Week	Ref.[3,43-47]
$1/\gamma$	Infectious period of dominant infection	2	1–2	Week	Ref.[47-49]
$1/\gamma'$	Latent infection period	2	1–2	Week	-
f	Case fatality rate	Based on actual mortality rates in different years	-	1	China CDC Information System
b_{r1}	Birth rate of people	Based on actual data	-	1	Statistical Yearbook of Anhui Province
d_{r1}	Mortality rate of people	Based on actual data	-	1	Statistical Yearbook of Anhui Province
Ticks					
$\beta_{2\text{-}1}$	Coefficient of tick-to-human transmissibility	$8\beta_1$	-	$(\text{Person*week})^{-1}$	Ref.[50]

$\beta_{2\text{-}3}$	Coefficient of tick-to-host infection	$8\beta_1$	-	$(\text{Pieces*week})^{-1}$	Ref.[50]
$1/\omega_2$	Incubation period of ticks	1	0–1	Week	Ref.[51,52]
b_{r2}	Birth rate of ticks	0.17321	-	1	Ref.[53]
d_{r2}	Mortality rate of ticks	0.01155	-	1	Ref.[53]
Host animals					
$\beta_{3\text{-}1}$	Coefficient of transmissibility rate of host animal to human	$2\beta_1$	-	$(\text{Person*week})^{-1}$	Ref.[50]
$\beta_{3\text{-}2}$	Coefficient of host animal infection to ticks	$8\beta_1$	-	$(\text{Pieces*week})^{-1}$	Ref.[50]
$1/\omega_3$	Host animal incubation period	1.71	0–12	Week	Ref.[54,55]
b_{r3}	Birth rate of host animals	0.04619	–	1	Ref.[53]
d_{r3}	Mortality rate of host animals	0.00231	–	1	Ref.[53]

Table 1: are there any uncertainties among these estimates of model parameters? If yes, how robust are your conclusions? Some probabilistic sensitivity analyses should be conducted.

Author's Response：

We thank the reviewer for highlighting the issue of parameter uncertainty and the need to assess how stable our conclusions are under different plausible parameter values. We fully agree that explicitly presenting probabilistic sensitivity analyses is important, and in the revised version we have added these results to evaluate the robustness of our findings.

We agree that uncertainties do exist in model parameter estimates. To address this concern more directly, we revised both the Methods and Results to clarify our sensitivity analysis design and to present the corresponding findings. We added a range column in Table 1 to report plausible values for key parameters, and we conducted a probabilistic sensitivity analysis (PSA) and partial rank correlation coefficient (PRCC) analysis to evaluate the stability of our conclusions under joint parameter uncertainty. The additional results indicate that only a small subset of transmission-related parameters shows relatively large influence on Re, while most other parameters contribute limited variability, supporting the robustness of our main qualitative conclusions.

For clarity, we list the new or revised text added to the manuscript below:

Revised version: Lines 808-818; Clean version: Lines 609-619：

4.4.3 Sensitivity Analysis

We assessed the robustness of our results to parameter uncertainty using a probabilistic sensitivity analysis (PSA) and partial rank correlation coefficient (PRCC) analysis. The PSA was implemented using standard Monte Carlo sampling, in which key uncertain parameters were jointly sampled within plausible ranges and the effective reproduction number was recalculated for each draw to obtain the uncertainty distribution of R_e. We performed 5,000 Monte Carlo draws for each analysis. To complement this uncertainty propagation, we computed PRCCs to quantify the relative influence of individual parameters on Re while controlling for the simultaneous variation of the remaining parameters, thereby identifying the parameters that most strongly contribute to variability in R_e.

Revised version: Lines 435-442; Clean version: Lines 243-250：

To evaluate the robustness of these city-level transmissibility patterns to parameter uncertainty, we further conducted sensitivity analyses. The PRCC-based global sensitivity results for Anhui Province by region and year are provided in Fig. S2, showing that the variability in Re is primarily driven by a limited subset of key transmission-related parameters. In addition, the probabilistic sensitivity analysis for Anhui Province and the five high-incidence cities during 2019–2023 is shown in Fig. S3, which presents the uncertainty distributions of Re and supports the stability of the temporal and spatial patterns reported in Fig. 5.

Supplementary Material:

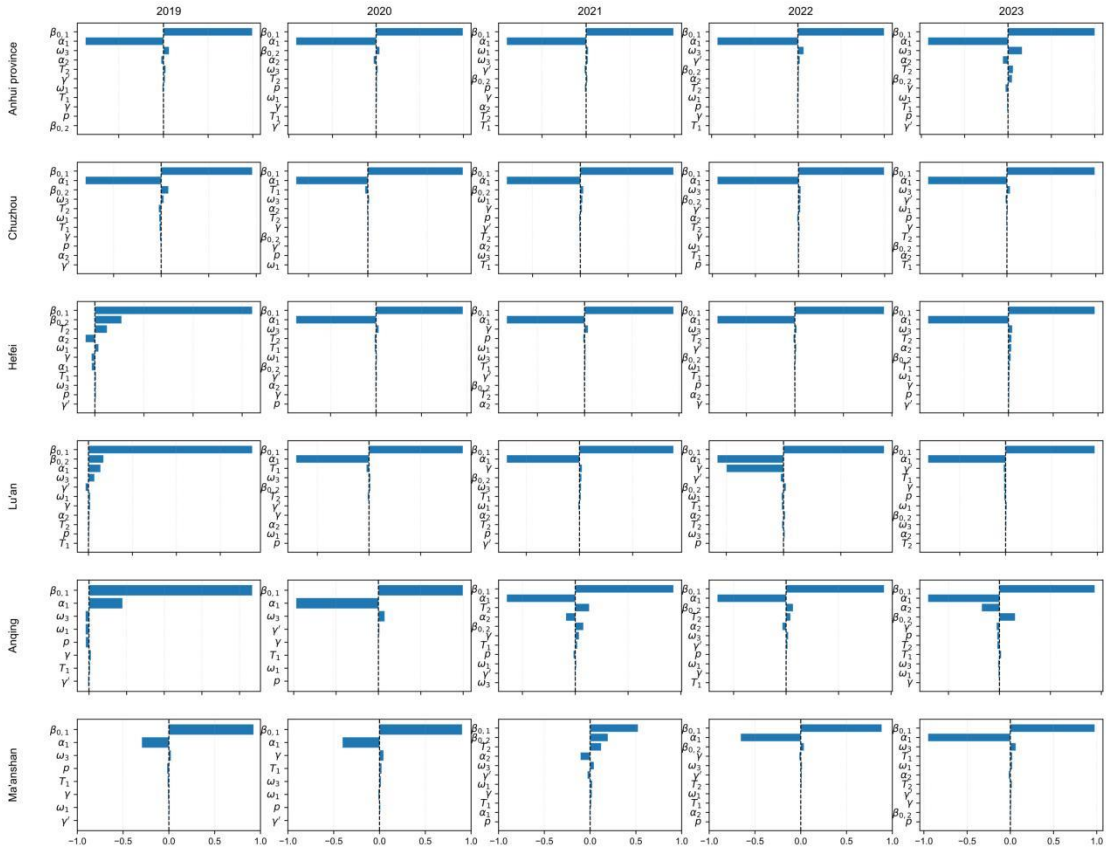

Figure S2 Global sensitivity of the effective reproduction number (R_e) to key model parameters based on PRCC, by region and year, Anhui Province

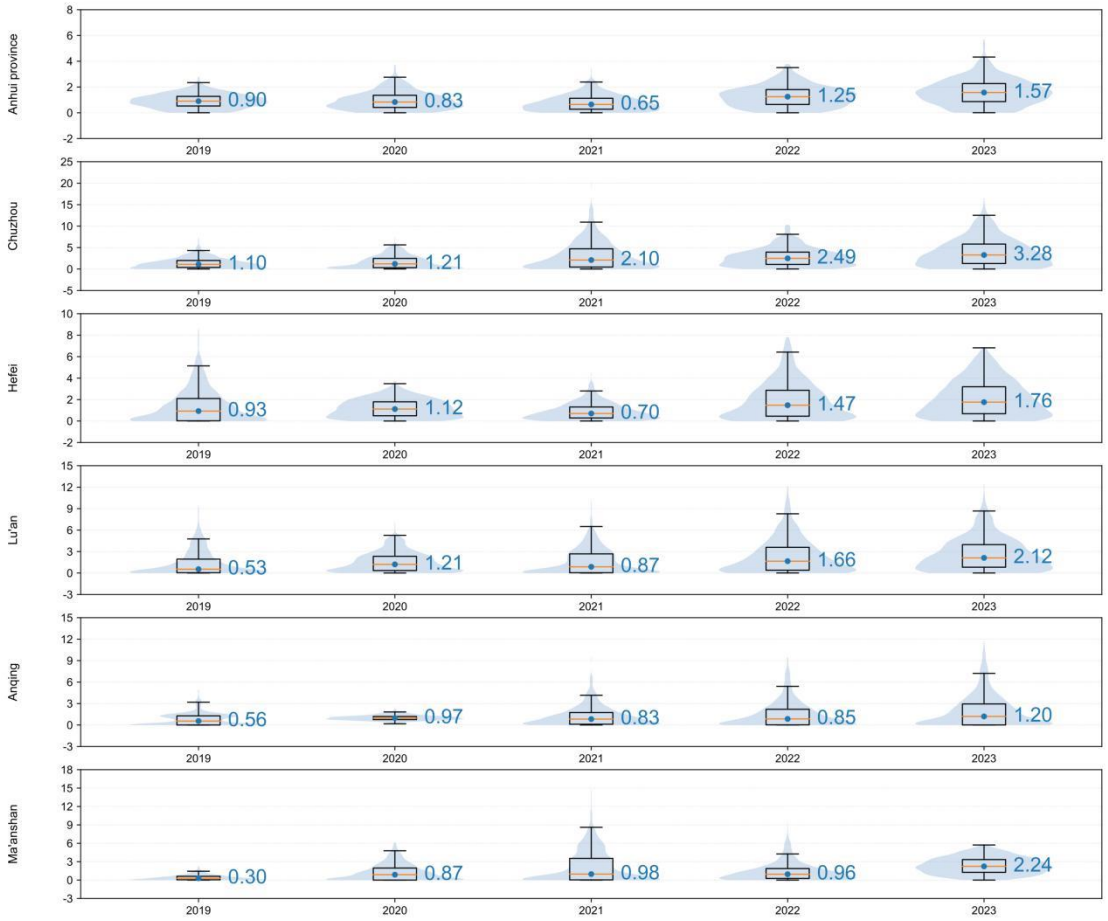

Figure S3 Probabilistic sensitivity analysis of the effective reproduction number (R_e) for SFTS in Anhui Province and the five high-incidence cities, 2019–2023

Table 2: the values listed in the last row are not all “Total”
The uncertainty in “Total” should be listed.

Author’s Response：

We thank the reviewer for carefully checking Table 2. In the original version, the last row was labelled “Total” and combined cumulative counts with overall summary measures, which could indeed be confusing and raised the question of uncertainty around these values.

In the revised manuscript, we have added detailed annotations and explanations to the last row of Table 2 to ensure that the meaning of each indicator is accurately conveyed. In addition, we have also supplemented the uncertainty intervals.

We have rearranged the structure of the manuscript, with Table 2 now renumbered as

Table 1.

Revised version: Lines 316-318; Clean version: Lines 149-151：

Table 1. Overview of reported cases of severe fever with thrombocytopenia syndrome in Anhui Province, 2019–2023.

Year	Number of cases	Incidence rate (/100,000)	Number of deaths	Case fatality rate (%)	Number of prefecture-level cities	Number of counties/districts
2019	443	0.7272(0.6595,0.7949)	16	3.6117(1.8742,5.3492)	12	56
2020	641	1.0500(0.9687,1.1312)	39	6.0842(4.2337,7.9348)	13	62
2021	543	0.8883(0.8136,0.9630)	11	2.0258(0.8408,3.2108)	14	63
2022	841	1.3726(1.2798,1.4654)	22	2.6159(1.5372,3.6947)	12	62
2023	1415	2.3117(2.1913,2.4322)	33	2.3322(1.5458,3.1185)	13	68
Accumulation*	3883	1.2707(1.2307,1.3107)	121	3.1161(2.5696,3.6627)	14	83

Accumulation*:
1."Number of cases" and "Number of deaths" (Accumulation*): Aggregate totals of annual data from 2019–2023.
2."Incidence rate (/100,000)" and "Case fatality rate (%)" (Accumulation*): Period average rates, calculated as total cases / total population for 2019–2023 and total deaths / total cases for 2019–2023, respectively.
3."Number of prefecture-level cities" and "Number of counties/districts" (Accumulation*): All regions involved from 2019 to 2023
4."()": 95% confidence intervals (95% CI) = $p \pm 1.96 \cdot \sqrt{[\, p(1-p) \,/\, n \,]}$

Could the high incidence from 2023 be linked to the NPIs against COVID-19 in China?

Author's Response：

We thank the reviewer for this thoughtful comment. This is an important and timely question, and we consulted relevant national and international evidence to better

contextualize the unusually high SFTS incidence observed in 2023. The high SFTS incidence observed in 2023 may plausibly be linked, at least in part, to the broader public health context surrounding COVID-19-related non-pharmaceutical interventions (NPIs) and their subsequent relaxation. Although SFTS is a tick-borne disease and not directly targeted by respiratory-focused measures, national and regional evidence suggests that COVID-19 NPIs were associated with reductions in the reported incidence of many notifiable infectious diseases during periods of strict control, with rebounds observed for some conditions as interventions were eased. This context raises the possibility that indirect changes in population mobility, outdoor activity patterns, healthcare-seeking behavior, and surveillance sensitivity may have contributed to the 2023 increase in reported SFTS incidence.

We have added additional discussion to acknowledge this possibility, outline the potential indirect mechanisms relevant to SFTS, and emphasize that this interpretation is presented as a plausible contributing contextual factor rather than a definitive causal explanation.

Revised version: Lines 509-514; Clean version: Lines 313-318：

In addition, the elevated incidence in 2023 may also be interpreted in the broader post-COVID-19 context. Although SFTS is a tick-borne disease and not directly targeted by respiratory-focused NPIs, the relaxation of COVID-19-related measures may have indirectly increased exposure opportunities through changes in outdoor activity patterns, occupational behaviors, inter-regional mobility, and healthcare-seeking and reporting practices.

Revised version: Lines 528-531; Clean version: Lines 330-333：

Taken together, these observations suggest that the recent temporal changes in SFTS burden may reflect the combined effects of surveillance improvement, ecological expansion of vectors and hosts, climatic influences, and broader societal and healthcare dynamics following the COVID-19 period.

Reviewer #2 (Remarks to the Author):

This is a very good manuscript that describes a new model for SFTS in China. This disease is undergoing a rapid expansion and needs better study, so this paper is very

timely. The authors do a very good job of presenting much of the information and results. I have only a couple majors comments and a few minor corrections to suggest.

Major comments.

I am a bit concerned about the minimal amount of information in the text about the tick vector itself. Since this population is included in the equations, I would suggest that there is a need to have a bit more about the biology of this tick species and its life history described in the introduction. For example, what is known about any recent changes in this ticks geographic range or population density? With a weekly time step, the tick life history dynamics might play a larger role than is currently included with this model.

Author's Response：

We sincerely thank the reviewer for these valuable comments, which have helped address the gaps in our study. As you suggested, we have enhanced the Introduction section by adding information on the animal hosts and transmission patterns of SFTS, while highlighting the primary vector (ticks) and their expanding activity range in China.

Revised version: Lines 75-91; Clean version: Lines 65-81：

Ticks, including species such as *Haemaphysalis longicornis* and *Haemaphysalis flava*, are established as the primary vectors for SFTSV transmission. *Haemaphysalis longicornis* is extensively distributed and potentially affects 588 million people across 1,140 counties in China. Furthermore, its distribution range within China may be continually expanding. Study has demonstrated that all developmental stages of *H. longicornis* can acquire SFTSV by infecting animals through biting, and subsequently transmit the virus back to naive animals during blood-feeding. Following SFTSV infection at any single developmental stage, transstadial transmission of the virus to the subsequent developmental stage was observed. Female adult ticks are capable of vertical virus transmission via the transovarial route. Collectively, these results confirm that SFTSV can undergo both transstadial and transovarial transmission, thereby establishing a complete transmission cycle spanning the *H. longicornis* larvae–nymphs–adults life cycle and animal hosts. Additionally, the virus also exhibits a broad animal host tropism, infecting species such as cats, cattle, sheep, and hedgehogs, thereby establishing a risk of zoonotic transmission. Evience of human-to-human

spread has also been documented. The extensive host range coupled with multiple transmission pathways presents a multifaceted challenge for public health control efforts.

“With a weekly time step, the tick life history dynamics might play a larger role than is currently included with this model.” This question goes to the core of how biological realism and data-supported model structure are balanced in a multi-population framework. The tick life cycle and stage-specific blood-feeding behavior can influence the timing and intensity of SFTSV transmission, and a weekly time scale places attention on whether these processes are represented in a sufficiently clear and biologically grounded way. In the revised manuscript, we have strengthened and clarified our description of how tick life history is incorporated in the MMDM. We refined the text in Section 4.3 Construction of the Multi-Population and Multi-Route Dynamic Model (MMDM), updated Fig. 7, and added Supplementary Material Appendix Fig. S5 to provide a clearer biological basis for the tick component. The revised description explains more explicitly that our tick representation is intended to incorporate the combined contribution of the three blood-feeding stages (larva, nymph, and adult), consistent with our original modelling intent, and we now present this rationale more clearly for readers. We also added an explanation for adopting a weekly time step. While we aimed to use a relatively fine temporal resolution, daily case reports in our setting are too sparse and unstable for robust fitting and inference; thus, weekly aggregation provides a practical balance that improves signal-to-noise while still capturing seasonality and the key cross-population transmission dynamics.

To clarify the representation of tick life history and the rationale for the weekly time step, we made the following revisions:

Revised version: Lines 678-684; Clean version: Lines 479-485：

(3) The tick population in the present model represents an integrated framework across the three blood-feeding life stages (larva, nymph, and adult). Rather than modelling each stage separately, we synthesise their contributions into the tick compartments to reflect the overall transmission potential of ticks while keeping the model structure parsimonious and stable. A schematic of the three-stage tick life cycle is provided in Supplementary Material Appendix Fig. S5.

Revised version: Line 692; Clean version: Line 493：

Fig. 7. The MMDM for SFTS among the human, tick, and animal host populations.

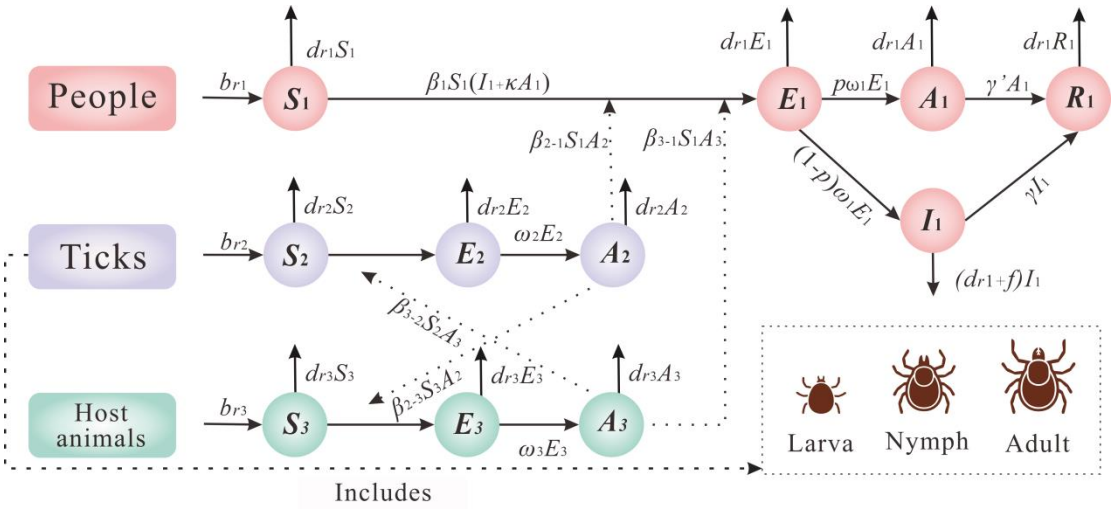

Supplementary Material:

Fig. S5. Three-host life cycle of ticks highlighting the larval, nymphal, and adult blood-feeding stages:

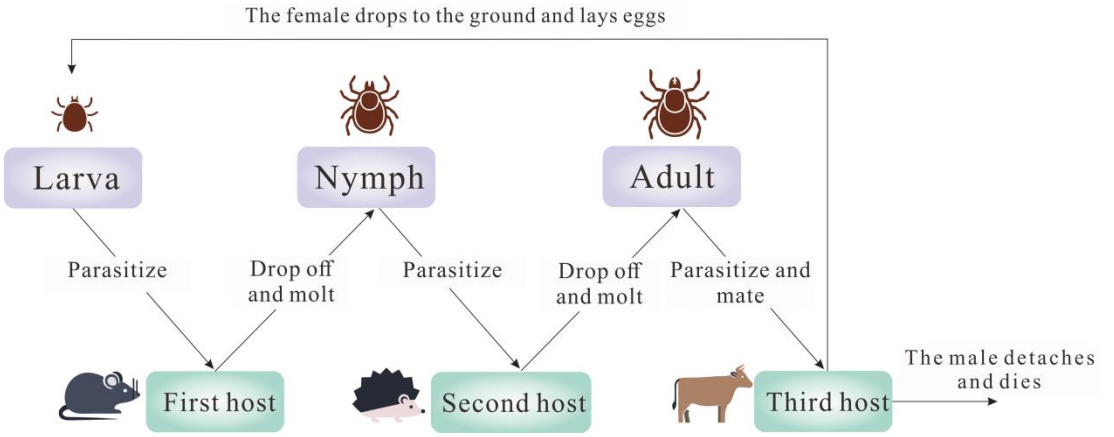

Figure S5 Life cycle of ticks highlighting the larval, nymphal, and adult blood-feeding stages. Larvae, nymphs, and adult ticks feed sequentially on first, second, and third hosts, with molting occurring after detachment between stages; adult females drop to the ground to lay eggs, completing the life cycle. The “first host”, “second host”, and “third host” represent generalized host categories across the tick’s developmental blood-feeding sequence. The animals illustrated in the diagram are for conceptual visualization only and do not indicate specific or exclusive host species in this study.

Figure 3 and 4 are overly complicated. While I appreciate the amount of information provided, there is so much there it is overwhelming and impossibly small font. I would recommend the authors either divide up the information into a series of figures or move some of these to the supplemental information. Either way, these need to be simplified. Additionally, all figures should have more information in the captions to tell the reader what is being shown and the interpretations of those findings.

Author's Response：

We appreciate the reviewer's valuable feedback regarding the figures. In response to the raised concerns, we have made corresponding revisions to the figures.

Specifically, we simplified the contents of figure 3 and figure 4 as suggested to better highlight the key findings:

For figure 3, we removed subplot A (representing incidence and fatality rates) and subplot D (depicting occupational distribution), since the same information has already been presented in table 2 and table S1. Meanwhile, subplots E–I were eliminated, and the more intuitive and concise subplot D was adopted to present the equivalent information on spatiotemporal distribution and seasonality.

For figure 4, subplot D was removed because the information it conveyed overlapped with that of subplot C.

In addition, we supplemented the key information in the legends of figure 3 and figure 4 to facilitate readers' interpretation.

We have rearranged the structure of the manuscript, with Figures 3 and 4 now renumbered as Fig 1 and 2 respectively.

Revised version: Line 322; Clean version: Line 153：

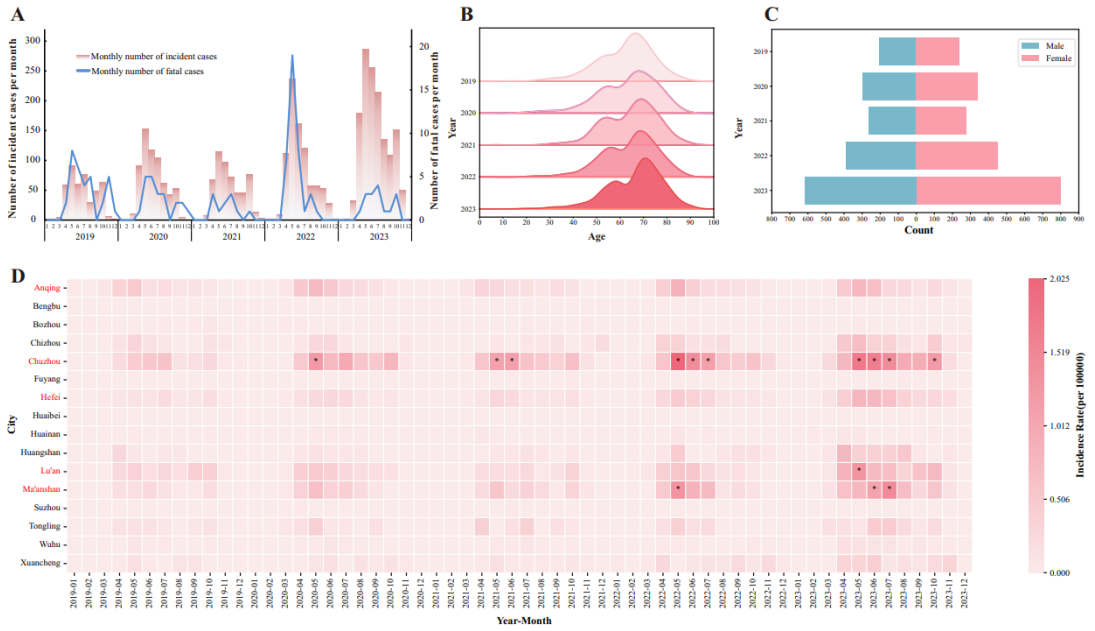

Fig. 1. Epidemiological characteristics of severe fever with thrombocytopenia syndrome in Anhui Province, 2019–2023. A: Monthly case counts and death tolls. B: Kernel density estimation of the age probability distribution. C: Sex distribution. D: Spatiotemporal heatmap of SFTS incidence at the prefecture-level city scale in Anhui Province. Cities marked in red represent the top five in terms of cumulative incidence from 2019–2023 (Chuzhou, Ma'anshan, Lu'an, Anqing, and Hefei). The asterisk (*) indicates an incidence rate ≥ 1.012 per 100,000 population.

Revised version: Line 354; Clean version: Line 176：

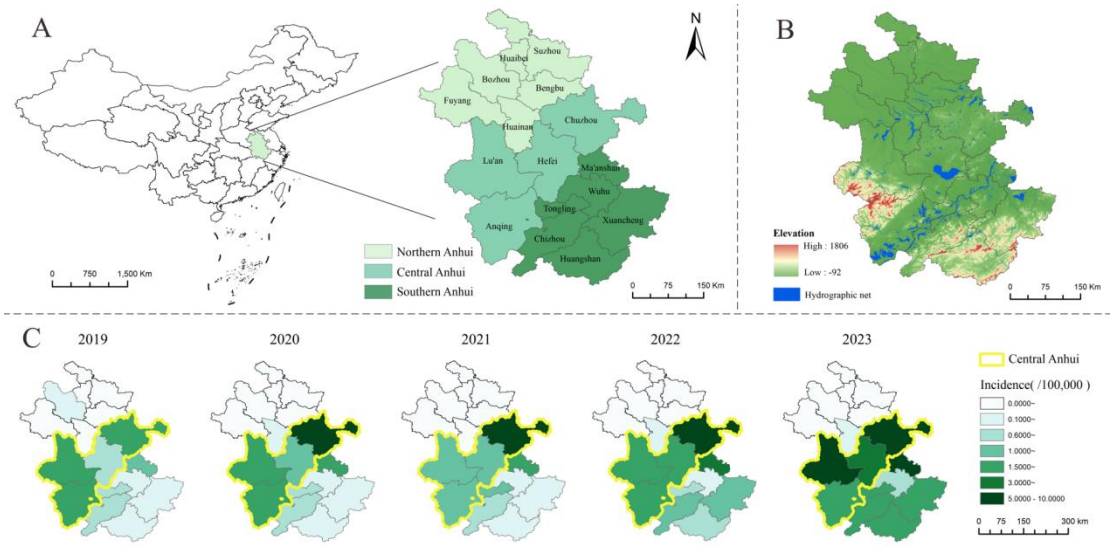

Fig. 2. Spatiotemporal distribution of SFTS in Anhui Province, 2019–2023. A:

The study area Anhui Province was divided into three regions, Northern Anhui (Suzhou, Huaibei, Bengbu, Bozhou, Fuyang, Huainan), Central Anhui (Hefei, Lu'an, Chuzhou, Anqing), and Southern Anhui (Tongling, Wuhu, Ma'anshan, Chizhou, Huangshan, Xuancheng). B: Map illustrating the topographic elevation and distribution of major water bodies in Anhui Province. C: Annual incidence rates of SFTS at the prefecture-level city scale for the years 2019 to 2023. The map was obtained from GaryBikini (https://zenodo.org/records/10624971). The digital elevation model (DEM) was obtained from the Resource and Environmental Science Data Platform (RESDC: https://www.resdc.cn/).

Other smaller comments.

The language of lines 330-333 is a bit confusing. I would suggest rewording to better explain that the drop of Re below one starts during the windows given. As it currently reads, it would seem that these were the only weeks that it was below 1.

Author's Response：

We thank the reviewer for pointing this out. Our intention was to indicate the time window during which R_e first crossed below 1 and then remained below 1 for the rest of the transmission season, rather than to imply that these were the only weeks with $R_e < 1$. We have revised the wording to remove this ambiguity. In addition, we have asked a native English-speaking editor to review the language and clarity of the entire manuscript to further improve readability and consistency.

Revised version: Lines 425-433; Clean version: Lines 237-242：

From 2019–2023, the reproduction number R_e for SFTS in Anhui Province decreased below 1 between weeks 24 and 28 and remained below 1 thereafter. Similar patterns were observed in the five high-incidence cities (Fig. S4). The R_e fell below 1 between weeks 28 and 31 in Chuzhou, weeks 25 and 30 in Hefei, weeks 24 and 27 in Anqing, weeks 27 and 32 in Lu'an, and weeks 28 and 30 in Ma'anshan, respectively, after which it remained below 1 for the remainder of the transmission season.

Spacing needs fixed in line 354.

Author's Response：

We thank the reviewer for noting this issue. The spacing at line 354 has been corrected in the revised manuscript, and we have also checked and standardised the spacing and related formatting in the surrounding text.

Numbering of list in lines 424-431 is not a usual numbering style.

Author's Response：

We thank the reviewer for this remark. We have revised the numbering style of the list in the indicated section to a conventional format in the updated manuscript.

Revised version: Lines 556-566; Clean version: Lines 357-367：

(1) Establish a dynamic monitoring network for tick density and the virus-carrying rate of animal hosts, and activate an early warning response before the vector's active season of the vector. (2) Conduct health promotion and education for high-risk occupational groups, including those engaged in farming and tea picking, on topics such as tick bite prevention techniques and post-exposure management procedures to reduce their exposure risk. Simultaneously, strengthen the capacity of primary health care institutions for early identification of SFTS cases to shorten the infectious period. (3) Carry out environmental management in peri-urban areas and regions with frequent population movement, reducing vector habitat suitability through vegetation management and livestock ectoparasite control.

Coloring for Figure 7 is a bit confusing. I associate green with Re < 1 and red with Re > 1 as some type of danger indication, but this seems to just be colored by region? It would be easier to interpret if the color scheme was based on the Re value.

Author's Response：

We sincerely thank the reviewer for this helpful suggestion. We agree that an R_e-based colour scheme improves interpretability and reduces potential confusion. In the revised manuscript, we have changed the colouring of Figure 7 from region-based colours to an R_e-based scale. The legend has been updated accordingly so that the colour gradient directly reflects the magnitude of Re, making the figure easier to interpret at a glance.

We have rearranged the structure of the manuscript, with Figures 7 now renumbered as Fig 5 respectively.

Revised version: Line 445; Clean version: Line 253：

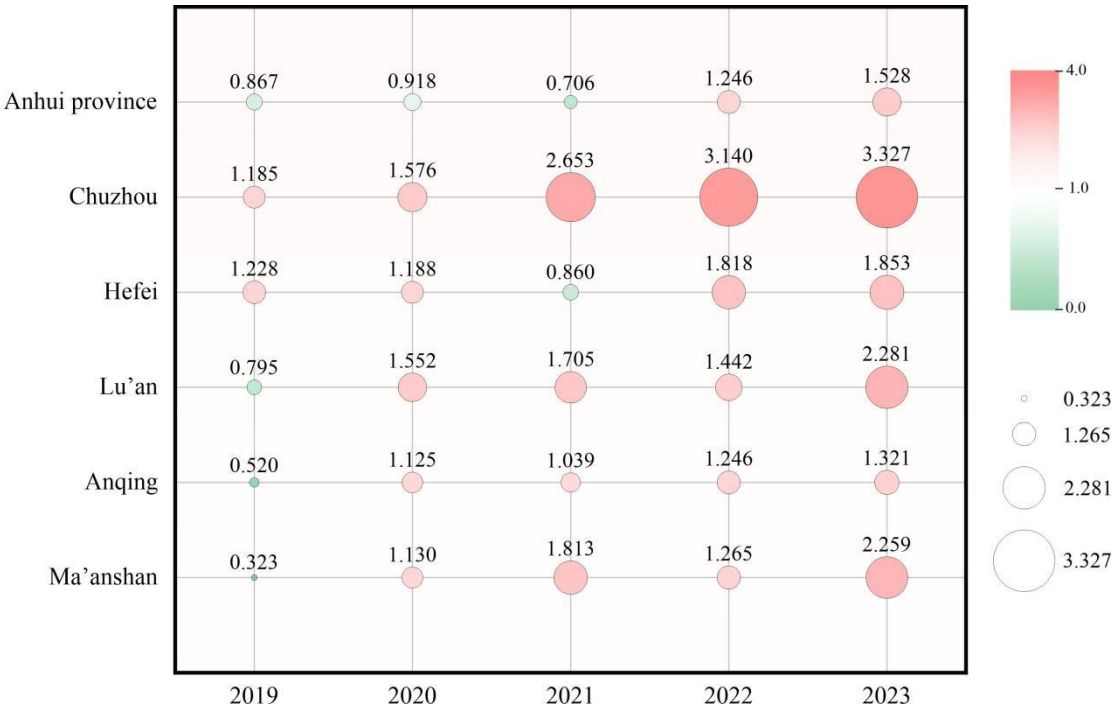

Fig. 5. Effective reproduction number (R_e) values for Anhui Province and the five cities with the highest incidence rates, 2019–2023. Circles are positioned by year (x-axis) and region (y-axis); the circle area is proportional to the yearly mean R_e. The green circles indicate R_e<1, whereas the red circles indicate R_e >1, with darker shades representing larger R_e values. The numeric labels above each circle show the exact yearly mean R_e.

We sincerely thank the reviewer once again for these insightful and constructive comments. We fully agree that the two issues raised are important for improving the transparency, interpretability, and epidemiological relevance of our work, and we have carefully revised the manuscript accordingly. Please find the comments and our responses reproduced below. Author responses are in blue.

Reviewer #1 (Remarks to the Author):

Thank authors for taking effort to thoroughly revise their manuscript. Although it improves in many aspects, I still have concerns about how they conducted model fit with many things unknown, for example

1/ Their formula for Re (actually R0 because they calculated it on the disease-free equilibrium) is involved with population size N1, N2 and N3. Without the values of these, how to calculate Re? if the values of N1, N2 and N3 were used, how were the populations estimated?

Author's Response：

We thank the reviewer for this insightful comment, which helped us to improve the clarity of our presentation and avoid potential misunderstandings regarding the definition of the reproduction number and the role of population-size–related parameters in the model. We agree that what was previously referred to as Re in the manuscript is evaluated at the disease-free equilibrium and therefore corresponds to the basic reproduction number R0. We have revised the terminology throughout the manuscript to ensure consistency and to avoid confusion.

With respect to the population-size–related parameters, N1, N2, and N3 play different roles in our framework. Specifically, N1 corresponds to the human population size and was fixed using official demographic statistics, which are well-defined and reliably measured. In contrast, N2 and N3 are pathway-scaling parameters that modulate the contributions of the corresponding transmission routes. Unlike N1, these quantities do not have direct empirical counterparts that can be reliably measured at the city or provincial level. For this reason, N2 and N3 were not assigned fixed values prior to analysis but were jointly estimated together with the transmission coefficients during model calibration. We note that this distinction was not sufficiently clearly described in the original version of the manuscript, and we have now revised the Parameter Fitting subsection of the Methods to explicitly clarify this point.

At the same time, the plausible ranges of N2 and N3 were constrained according to the scale of the human population N1 in each study area, in order to preserve realistic orders of magnitude and prevent implausible parameter combinations. This constraint reflects the expectation that the relative scales of different transmission pathways should remain consistent with the demographic context of each region, even though they are not directly observable.

In this study, we focus on R0 as the main epidemiological quantity of interest, which is a composite function of multiple model parameters, including N2 and N3. As in many compartmental transmission models, multiple combinations of transmission rates and pathway-scaling parameters may yield similarly good fits to the observed incidence data. While this implies that individual parameters may not be uniquely identifiable in isolation, the resulting values of R0 remain stable across such parameter combinations. For this reason, R0 provides a more robust and interpretable summary of transmission potential than any single parameter considered alone. To further assess how uncertainty in model parameters propagates to uncertainty in R0, we conducted a probabilistic sensitivity analysis using partial rank correlation coefficients (PRCC), which showed that N2 and N3 exert strong influence on R0.

To address this comment, we have revised the manuscript in several aspects. Specifically, we clarified the definition of the reproduction number and consistently referred to it as R0 throughout the manuscript. We also revised the Methods section to explicitly state that N2 and N3 are pathway-scaling parameters that were jointly estimated together with the transmission parameters, with their plausible ranges constrained according to the scale of N1 in each study area, rather than being treated as fixed demographic quantities (Revised version: Lines **599-618**; Clean version: Lines **589-607**). In addition, we expanded the sensitivity analysis in the Supplementary Material by explicitly including N2 and N3 as uncertain parameters and assessing their joint influence on R0 using PRCC (Supplementary Fig. S2).

Revised version: Lines 599-618; Clean version: Lines 589-607：

The human-to-human transmission coefficient β_1 is specified as a seasonal function of time and is parameterized by a baseline intensity, a phase parameter and a period. In the calibration procedure, the parameters governing the magnitude and timing of this seasonal pattern (denoted β_0 and α), together with the effective host population sizes associated with tick-mediated transmission pathways (N2 and N3), were treated as free parameters and jointly estimated.

The period T and all remaining natural-history parameters were fixed at the baseline values listed in Table 1. N1, representing the human population size, was fixed using official demographic statistics, whereas N2 and N3 were not directly observable and were therefore treated as composite parameters reflecting effective host availability and contact intensity rather than absolute census counts.

For each study area, the free parameters were estimated by nonlinear least squares, minimizing the sum of squared differences between the observed weekly incidence and the model-predicted weekly number of new symptomatic infections. The optimization was implemented in Python using the lmfit package, and convergence was assessed by the relative change in the objective function. The goodness-of-fit of the calibrated model is summarized in the Results and in Supplementary material Appendix Table S5 using the coefficient of determination (R2), mean squared error (MSE), and mean absolute error (MAE) between observed and model-predicted weekly cases.

Supplementary Fig. S2:

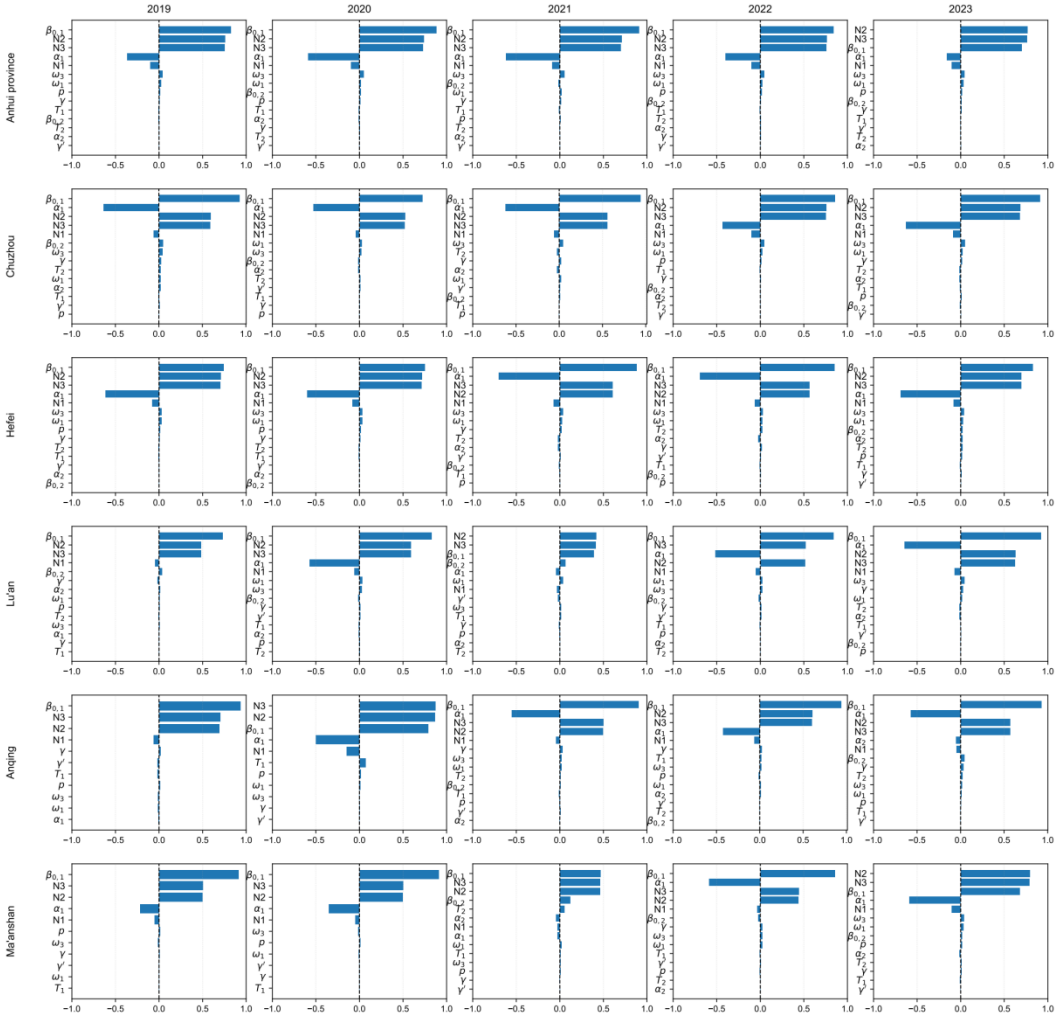

Fig. S2 Global sensitivity of the basic reproduction number (R_0) to key model parameters based on PRCC, by region and year, Anhui Province

2/ as humans can be infected via contact with humans, ticks and animals, what are the corresponding proportions of the infections? Does this agree with the data listed in Table 2? This knowledge may provide some key information for the control of the disease.

Author's Response：

We sincerely thank the reviewer for raising this important point. We fully agree that understanding the relative contributions of different transmission pathways is key

information for disease control, as it directly informs which intervention strategies are likely to be most effective. This suggestion provided a valuable direction for improving the public health relevance of our work, and we have followed it to strengthen both the interpretation and the presentation of our results.

The exposure history summarized in Table 2 is based on retrospective epidemiological investigations and records possible contact scenarios prior to symptom onset, including outdoor activities, tick exposure, animal contact, and contact with symptomatic individuals. These data provide important contextual information about the environments and behaviors in which infections may have occurred, but they are also subject to possible recall bias. At the same time, these variables are not mutually exclusive, and a single individual may report multiple types of exposure. In addition, a substantial proportion of responses fall into the "unknown" category for several items. As a result, these data primarily offer descriptive clues regarding potential exposure risks rather than establishing definitive causal relationships..

Our transmission model is designed to characterize population-level transmission dynamics. The three pathways included in the model—human-to-human transmission, tick-mediated transmission, and animal-related transmission—enter the system through distinct transmission terms and jointly shape the overall transmission potential. Rather than assigning individual cases to specific exposure routes, the model captures how strongly each pathway contributes to sustaining transmission over time.

Following the reviewer's suggestion that this information is particularly relevant for disease control, we sought to provide a clearer and more quantitative summary of pathway-specific contributions. Specifically, we decomposed the model-predicted incidence into pathway-specific components and calculated their relative contributions to the total transmission potential for each region and year. These quantities describe the structural importance of each pathway in the modeled system, rather than the proportion of observed cases attributable to that pathway.

When aggregated across all regions and years, the relative contributions were approximately 14.7% for human-to-human transmission, 56.3% for tick-mediated transmission, and 29.0% for animal-related transmission. These results indicate that tick-mediated transmission plays a dominant role in sustaining transmission, followed by animal-related transmission, while human-to-human transmission contributes to a lesser extent.

Although these model-based contributions are not intended to be interpreted as case-attribution proportions, they are broadly consistent with the epidemiological patterns suggested by the exposure-history data. In Table 2, a large fraction of cases

reported rural or mountainous residence, outdoor activities, potential tick presence, and animal-related exposures, whereas direct contact with symptomatic individuals was relatively uncommon. This qualitative agreement helps to bridge the individual-level exposure data with the population-level transmission structure captured by the model.

From a disease-control perspective, these findings suggest that interventions targeting tick exposure and animal–tick–human interfaces are likely to be particularly impactful for reducing overall transmission potential. Such measures may include environmental management, tick control strategies, personal protective behaviors during outdoor activities, and targeted interventions for high-risk occupational groups. We have now highlighted these implications more explicitly in the Discussion, following the reviewer's suggestion.

To address this comment, we have revised the manuscript in two main ways. First, we added a clearer explanation of the conceptual distinction between retrospective exposure histories and model-based pathway contributions, together with a qualitative comparison between Table 2 and the modeled transmission structure (Revised version: Lines **364-378**; Clean version: Lines **360-374**). Second, following the reviewer's suggestion, we expanded the Supplementary Material to include a pathway-level decomposition of the model outputs, reporting the relative contributions of human-to-human, tick-mediated, and animal-related pathways to the overall transmission potential for each region and year (Revised version: Lines **254-258**; Clean version: Lines **251-255**; Supplementary Table S6-S7).

Revised version: Lines 364-378; Clean version: Lines 360-374：

The exposure history data (Table 2) in this study were collected through cross-sectional epidemiological surveys and should be interpreted with caution due to potential recall bias. These data primarily offer descriptive clues regarding potential exposure risks rather than establishing definitive causal relationships. In contrast, the model constructed in this study estimated the case contributions attributable to different pathways by quantifying their transmissibility, providing results that are closer to causal inference. Consequently, the exposure proportions derived from questionnaires (e.g., reported tick exposure, animal contact, or human contact) cannot and should not be directly equated or compared in numerical terms with the model-estimated contributions of each pathway (tick-borne, animal-associated, and human-to-human transmission). Nevertheless, it is noteworthy that both types of analyses are consistent in revealing the relative importance of the main transmission routes: both indicate that tick bites constitute the most significant transmission pathway for SFTS, followed by

contact with animals, while human-to-human transmission plays a relatively limited role.

Revised version: Lines 254-258; Clean version: Lines 251-255

To provide additional insight into the relative importance of different transmission routes, we summarized the model-estimated contributions of human-to-human, tick-mediated, and animal-related pathways. The aggregated proportions at the provincial level and their spatiotemporal variations across cities and years are presented in Tables S6–S7.

Supplementary Table S6-S7:

Table S6 Model-estimated relative contributions of different transmission pathways in Anhui Province (2019–2023)

Pathway	Total contribution	Percentage (%)
Human-to-human	441.64	14.70%
Tick-mediated	1690.24	56.30%
Animal-related	872.27	29.00%
Total	3004.14	100.00%

Table S7 Spatiotemporal variation in the relative importance of different transmission pathways across cities in Anhui Province (2019 − 2023)

Region	Year	Human (%)	Tick (%)	Animal (%)
Anhui	2019	13.19	69.58	17.23
Anhui	2020	15.58	54.10	30.32
Anhui	2021	14.46	50.09	35.45
Anhui	2022	19.47	67.41	13.13
Anhui	2023	23.66	56.12	20.21
Anqing	2019	11.48	62.52	26.01
Anqing	2020	12.27	56.84	30.89
Anqing	2021	4.94	39.20	55.86
Anqing	2022	6.49	38.38	55.13
Anqing	2023	6.67	40.95	52.38
Chuzhou	2019	5.53	42.18	52.29

Chuzhou	2020	13.54	33.97	52.49
Chuzhou	2021	7.80	48.23	43.97
Chuzhou	2022	9.75	72.05	18.20
Chuzhou	2023	10.62	52.30	37.08
Hefei	2019	5.20	39.82	54.98
Hefei	2020	8.97	42.98	48.05
Hefei	2021	8.82	38.38	52.80
Hefei	2022	11.53	38.94	49.53
Hefei	2023	15.70	43.53	40.77
Lu'an	2019	13.96	24.77	61.27
Lu'an	2020	6.53	48.76	44.71
Lu'an	2021	8.42	28.33	63.25
Lu'an	2022	6.47	48.67	44.86
Lu'an	2023	8.79	47.49	43.72
Ma'anshan	2019	4.10	27.95	67.95
Ma'anshan	2020	8.00	28.38	63.62
Ma'anshan	2021	6.42	27.72	65.86
Ma'anshan	2022	9.99	29.12	60.88
Ma'anshan	2023	11.06	36.47	52.47

We thank the reviewer for raising this remaining point of clarification. We agree that our previous wording did not make the estimation procedure for N2 and N3 sufficiently transparent. In response, we have revised the manuscript to describe more explicitly how these parameters were jointly fitted, how their bounds were imposed during optimization, and how this procedure is illustrated in the Supplementary Material. The reviewer′s comment and our response are presented below. Author responses are shown in blue.

Reviewer #1 (Remarks to the Author):

The authors have satisfactorily addressed my second concern, but I am still not clear how N2 and N3 are jointly estimated. In the revised version, they stated
"In the calibration procedure, the parameters governing the magnitude and timing of this
seasonal pattern (denoted β0 and α), together with the effective host population sizes associated with tick-mediated transmission pathways (N2 and N3), were treated as free parameters and jointly estimated"

for this they justified as
"...the plausible ranges of N2 and N3 were constrained according to the
scale of the human population N1 in each study area, in order to preserve realistic orders of magnitude and prevent implausible parameter combinations"

" N2 and N3 are pathway-scaling parameters that were jointly
estimated together with the transmission parameters, with their plausible ranges constrained according to the scale of N1 in each study area, rather than being treated as fixed demographic quantities"

If constrained, they could not be free.
Even if "jointly estimated", I cannot follow how this was done.

Author's Response：

We thank the reviewer for this important comment. We agree that our previous wording was not sufficiently precise and may have caused confusion. In particular, describing N_2 and N_3 as "free parameters" while also stating that their plausible ranges were constrained was imprecise. In the actual implementation, N_2 and N_3 were not treated as unconstrained free parameters. Rather, they were included in the fitted parameter vector together with the seasonal transmission parameters and were estimated simultaneously under prespecified lower and upper bounds.
More specifically, for each study area, the parameter set to be calibrated was (β_0, α, N_2, N_3). These four parameters were jointly estimated by nonlinear least squares using the lmfit package, by minimizing the sum of squared differences between the observed weekly incidence and the model-predicted weekly number of new symptomatic infections. Thus, "jointly estimated" means that N_2 and N_3 were optimized in the same calibration procedure and objective function as β_0 and α, rather than being assigned fixed values in advance or estimated in a separate step.

We also clarify that, in the code, explicit bounds were imposed on N_2 and N_3 during optimization. The imposition of these specific boundaries is both mathematically necessary and epidemiologically reasonable. As shown in our demographic data (Supplementary Table 1), SFTS infections predominantly occur among farmers. Since this high-risk agricultural group constitutes only a specific fraction of the total human population (N_1), the effective abundance of ticks (N_2) and animal hosts (N_3) that actively interact with humans should logically scale with the size of this specific farming sub-population, rather than the entire census population of the province or city. Without such constraints, the optimization algorithm might converge on mathematically optimal but biologically implausible values (e.g., approaching infinity or zero). Specifically, for Anhui Province, both N_2 and N_3 were bounded between 10^3 and 10^6. For the other five prefecture-level study areas, N_2 was bounded between 10^3 and 10^5, and N_3 was bounded between 10^3 and 10^4. Therefore, N_2 and N_3 should be understood as bounded fitted parameters rather than unconstrained free parameters.

In addition, we have revised the description of these parameters to make their interpretation clearer. N_1 denotes the human population size and was fixed using official demographic statistics. By contrast, N_2 and N_3 are not direct census quantities; they represent the effective abundance of ticks and animal hosts involved in transmission, respectively, while also capturing contact intensity relevant to transmission. For this reason, they were treated as effective population-scaling parameters and estimated during calibration within prespecified bounds.

We fully agree with the reviewer's underlying concern regarding the estimation of these parameters. In the absence of direct empirical data on tick and animal abundance, relying on joint estimation within biologically plausible bounds represents a limitation of our current study. We highly appreciate the reviewer's insightful critique, which highlights a crucial direction for our ongoing research. Notably, SFTS has recently been incorporated into the management of Class B infectious diseases in China. This major policy update will undoubtedly promote more systematic ecological and epidemiological surveillance nationwide, thereby providing richer and more reliable reference data in the near future. Moving forward, our research group plans to conduct targeted field investigations—such as systematic tick sampling and seroepidemiological surveys of domestic animals—to collect primary ecological data. These empirical data will fundamentally improve the parameterization of our transmission models and reduce reliance on mathematical constraints.

To further improve the transparency of the fitting procedure, we have added a schematic illustration in the Supplementary Material (Supplementary Fig. 6, "Workflow of joint parameter estimation and model calibration"), which visually summarizes how the parameter set was jointly fitted and how the model calibration was performed. We hope this additional figure helps readers more easily follow the estimation procedure.

We have revised the Parameter Fitting subsection of the Methods to explicitly describe: (1) which parameters were estimated simultaneously, (2) that N_2 and N_3 were optimized under bounded constraints rather than treated as unconstrained free parameters, (3) the specific bounds used for Anhui Province and the five prefecture-level study areas, and (4) the newly added workflow diagram in Supplementary Fig. 6 to aid interpretation of the calibration procedure.

Revised version: Lines 811-855; Clean version: Lines 593-629:

4.4.1 Parameter Fitting

Parameter fitting was conducted in Python 3.10.13 using NumPy 1.24.4 for numerical computations, SciPy 1.13.1 for ODE solving (solve_ivp), and lmfit 1.3.4 for model fitting. Given the low and highly sporadic daily number of reported SFTS cases in Anhui Province, the surveillance data were aggregated to weekly incidence to reduce stochastic noise and obtain a smoother epidemic trajectory. The weekly number of confirmed human SFTS cases in each study area was used as the calibration target. The deterministic model was integrated with a fourth-order Runge–Kutta scheme using a weekly time step and a relative tolerance of 0.001. The workflow of the parameter fitting procedure is shown in Supplementary Fig. 6.

The human-to-human transmission coefficient β_1 was specified as a seasonal function of time and is parameterized by a baseline intensity, a phase parameter and a period. In the calibration procedure, the parameters governing the magnitude and timing of this seasonal pattern (denoted β_0 and α), together with the effective population-scaling parameters associated with tick-mediated transmission pathways (N_2 and N_3), were estimated simultaneously.

The period T and all remaining natural-history parameters were fixed at the baseline values listed in Table 1. N_1, representing the human population size, was fixed using official demographic statistics, N_2 represents the effective abundance of ticks involved in transmission, and N_3 represents the effective abundance of animal hosts. Unlike N_1, which was fixed according to official demographic statistics, N_2 and N_3 were treated as calibration parameters rather than fixed empirical quantities. Their admissible ranges were prespecified for model calibration based on order-of-magnitude considerations and informed by the exposure-history distribution summarized in Table 2. Given that reported SFTS cases occurred predominantly among farmers, the size of the farming population in each study area was used as a practical reference for bounding N_2 and N_3. These constraints were introduced to confine the optimization to epidemiologically plausible values and to prevent unrealistic parameter combinations (Supplementary Fig. 6).

For each study area, the free parameters were estimated by nonlinear least squares using the lmfit package, minimizing the sum of squared differences between the observed weekly incidence and the model-predicted weekly number of new symptomatic infections. The optimization was implemented in Python using the lmfit package, and convergence was assessed by the relative change in the objective function. The goodness-of-fit of the calibrated model is summarized in the Results and in Supplementary Table 5 using the R^2, MSE, and MAE between observed and model-predicted weekly cases.

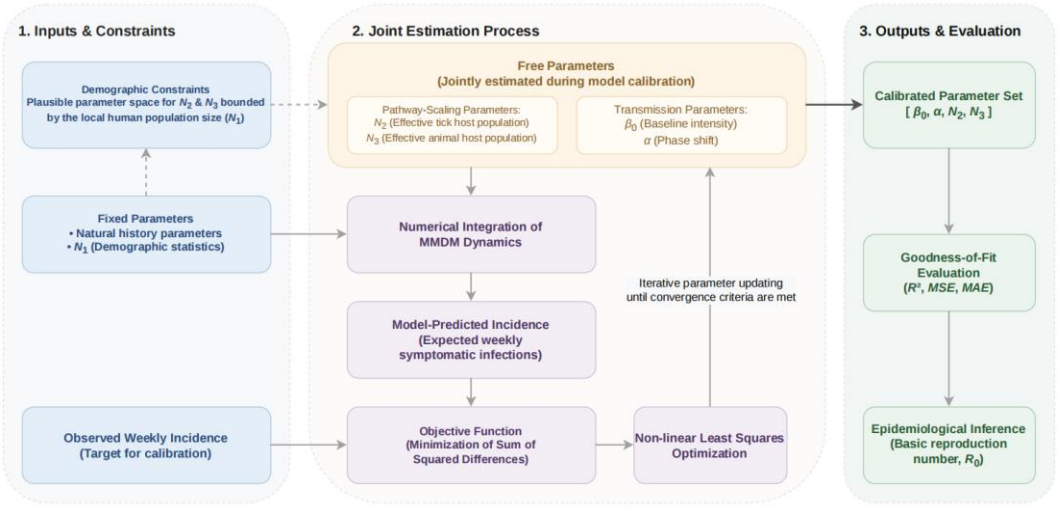

Supplementary Fig. 6. Workflow of joint parameter estimation and model calibration. Schematic of the joint parameter estimation framework. This flow diagram illustrates how the transmission parameters (β_0 , α) and the pathway-scaling parameters (N_2 , N_3) are treated as free parameters and jointly optimized. Notably, rather than fitting N_2 and N_3 in isolation or treating them as literal census counts, their plausible parameter space is explicitly bounded by the demographic constraint of the local human population size (N_1). This constraint ensures realistic effective contact intensities while avoiding implausible parameter combinations. The iterative non-linear least squares optimization loop minimizes the sum of squared differences between model-predicted incidence and observed data, ultimately yielding a stable and robust inference of the basic reproduction number (R_0). Specifically, for Anhui Province, both N_2 and N_3 were bounded between 10^3 and 10^6, whereas for the other five prefecture-level study areas, N_2 was bounded between 10^3 and 10^5 and N_3 between 10^3 and 10^4.